



# Modeling aerosol activation in a tropical, orographic, island setting: Sensitivity tests and comparison with observations

R.D. Russotto\*, T. Storelvmo, R.B. Smith

Department of Geology and Geophysics, Yale University, P.O. Box 208109, New Haven, CT 06520, USA

## ARTICLE INFO

### Article history:

Received 10 February 2013

Received in revised form 17 July 2013

Accepted 17 July 2013

### Keywords:

Aerosol

CCN

Orographic clouds

Tropics

Activation

## ABSTRACT

The aerosol, updraft and cloud droplet observations from the 2011 Dominica Experiment (DOMEX) field campaign provide an interesting opportunity to investigate the process of cloud droplet activation in a tropical, orographic, convective setting. This study involves adiabatic parcel model simulations with a state-of-the-art parameterization of droplet activation, which we run with aerosol size distributions and updraft velocities based on DOMEX data. We compare the cloud droplet concentrations predicted by the parameterization with the observations from DOMEX, and run various sensitivity tests to changes in model inputs on the order of their uncertainty, in order to gain insights into what factors are most important in determining the aerosol activation fraction in this setting. Our control simulations overestimated the observed droplet concentrations, especially for the days with strong trade winds, but in most cases these discrepancies could be eliminated by realistic changes in our assumptions. The remaining error could be the result of entrainment of sub-saturated air, precipitation, or advection of pre-existing clouds from upwind. We found strong sensitivities to the mean updraft velocity and to the size distribution and composition of particles in the Aitken mode, the smallest mode including particles below 100 nm. The Aitken mode accounted for 42% to 68% of the simulated droplet concentration in our control simulations, and simulations excluding the Aitken mode underestimated the observed droplet concentrations under realistic assumptions. Droplets from the Aitken mode dominated the changes in the simulated droplet concentrations in our sensitivity tests. The precision of our simulations, and our ability to constrain the role of the Aitken mode, were limited by our lack of knowledge of the composition and size distribution of Aitken mode particles, highlighting the importance of measuring these variables in field campaigns in similar settings.

© 2013 Elsevier B.V. All rights reserved.

## 1. Introduction

Cloud droplets form when aerosol particles become activated and begin unstable growth (Köhler, 1921). Changes in atmospheric aerosol composition, concentration and size distribution, e.g. due to anthropogenic emissions, can affect the concentration

and size distribution of cloud droplets. This, in turn, changes the clouds' reflectivity to shortwave radiation (Twomey, 1974) and their lifetime (Albrecht, 1989), affecting Earth's radiation budget. The effects of changes in aerosols on cloud shortwave reflectivity and cloud lifetime have been referred to as the first and second aerosol indirect effects, respectively, e.g. by Ramaswamy et al. (2001), or as the cloud albedo effect and cloud lifetime effect, e.g. by Lohmann and Feichter (2005). Since these effects are among the most uncertain components of the human impact on Earth's climate (Forster et al., 2007), simulation of the process of aerosol activation is of great interest to the climate modeling community.

\* Corresponding author at: Department of Atmospheric Sciences, University of Washington, 408 Atmospheric Sciences—Geophysics (ATG) Building, Seattle, WA 98195-1640, USA. Tel.: +1 206 543 4250; fax: +1 206 543 0308.

E-mail addresses: [russotto@u.washington.edu](mailto:russotto@u.washington.edu) (R.D. Russotto), [trude.storelvmo@yale.edu](mailto:trude.storelvmo@yale.edu) (T. Storelvmo), [ronald.smith@yale.edu](mailto:ronald.smith@yale.edu) (R.B. Smith).

Explicit simulation of cloud droplet activation is currently too computationally expensive for global climate models (GCMs), which have spatial resolutions too coarse to resolve clouds. Because of this, the process is often handled instead by parameterizations that estimate the activation fraction, the fraction of aerosol particles that become cloud droplet nuclei, using analytical expressions based on the basic controlling factors, including aerosol composition, size distribution, and updraft velocity. Ghan et al. (2011) provide a good summary of the parameterizations used in various GCMs and other weather and climate models. One of the most commonly used droplet nucleation parameterizations is that developed by Abdul-Razzak et al. (Abdul-Razzak et al., 1998; Abdul-Razzak and Ghan, 2000), hereafter referred to as the ARG parameterization.

The recently completed Dominica Experiment (DOMEX) field campaign, described in detail in Smith et al. (2012), provides an interesting opportunity to use droplet activation models in conjunction with observations to study the process of cloud droplet activation in a tropical, island, orographic setting. Here, aerosol size distribution and updraft velocity data collected during DOMEX are used as inputs to run an adiabatic parcel model that uses the ARG parameterization. We compare the resulting cloud droplet concentrations to the *in situ* observations made during DOMEX and test the sensitivity of the model results to changes in various inputs and assumptions on the order of their uncertainty. Doing this can provide insights into the factors controlling the activation fraction in this setting, and into the types of observational inputs necessary for accurately simulating aerosol activation.

## 2. Observations: the DOMEX campaign

During the DOMEX campaign, 21 research flights were flown over Dominica and the nearby ocean using the University of Wyoming King Air aircraft. The King Air had on board two optical aerosol instruments: the condensation particle counter (CPC), here referred to as the CN counter, and the Passive Cavity Aerosol Spectrometer Probe (PCASP-SPP200). The CN counter saturates particles with butanol before counting them, detecting particles as small as 10 nm in diameter without resolving size distributions, while the PCASP dries particles before measuring them (Strapp et al., 1992), obtaining a size distribution of particles between 95 nm and 2.991  $\mu\text{m}$  in diameter. Also on board were two optical cloud droplet spectrometers, the Forward Scattering Spectrometer Probe (DMT FSSP-100) and the Cloud Droplet Probe (DMT CDP).

Fig. 1 shows the locations and altitudes of the horizontal legs flown during the campaign. The most relevant legs to this study are Leg 1, which measured conditions upwind of the island, and Legs 3 and 4, which measured conditions over the island, including inside the orographic clouds, on the eastern and western sides, respectively. Legs 1L, at 300 m, and 1H, at 1200 m, were flown once per flight, and Legs 3 and 4 were flown 2 or 3 times each for the flights included in this study.

Smith et al. (2012) identified two major convective regimes during DOMEX: a strong trade wind regime, in which convection is triggered by forced ascent over Dominica's mountains, and a weak trade wind regime, in which convection

is thermally driven through diurnal heating of the island slopes. Fig. 2 shows a schematic of the two regimes. While convection occurs in both regimes, the low wind regime produces very little precipitation, so that there is almost no climatological diurnal cycle over Dominica. In the low wind regime, the air in Legs 3 and 4 has depleted  $\text{CO}_2$  compared to the oversea air, which is evidence of contact with the forested island surface. In the high wind regime, by contrast, there is no such depletion, indicating that the source air for the clouds is oceanic. The island-derived aerosols in the low wind regime have many more small particles, but fewer large particles, than the ocean-derived aerosols in the high wind regime (see the aerosol concentrations in Table 3). Research flights RF12, RF13, RF16, and RF17 are considered representative of the high wind regime, and RF07 and RF08 represent the low wind regime. For further discussion see Smith et al. (2012), particularly the section on island-derived tracers.

For the high wind flights, we run the model based on aerosol size distributions from Leg 1. An average of the leg averages for Legs 1L and 1H is used. There is some variation in the aerosol concentrations between Legs 1L and 1H, with generally higher concentrations closer to the surface. Using only Leg 1L or 1H instead of their average shifts the predicted droplet concentration by on the order of  $10 \text{ cm}^{-3}$ , except for RF12 where the aerosol concentrations in Legs 1L and 1H are very similar. The average is used partly because the amount of uplift would be expected to vary in the north–south direction given the uneven terrain, and also because, these being convective clouds, we would expect some vertical mixing. Updraft velocity and cloud droplet data from the high wind flights are taken from cloud penetrations in Leg 3, where the convection is strongest for these cases. See Section 6.2 for a discussion of observational uncertainties for the high wind cases arising from issues such as precipitation, entrainment, and contamination from upwind clouds.

For the low wind flights, we take aerosol data from detrainning air in Leg 4, and updraft velocity and cloud droplet measurements from cloud penetrations in Leg 4, where the convection is strongest for this regime. The use of detrainning air from the convection in Leg 4 for the aerosol source air presents the possible issue that the clouds could be scavenging out aerosols that were present in the original source air coming from the island slopes. However, since the low wind days did not have much precipitation, this effect is probably small.

For each flight, the measurements are averaged over all the data points in the relevant flight legs satisfying certain criteria for the liquid water content (LWC). For the aerosol data, we require that the LWC from both CDP and FSSP be less than  $0.003 \text{ g m}^{-3}$ , in order to exclude cloudy or precipitation-containing air. For the updraft velocity measurements, as well as cloud droplet concentrations for comparison with model results, we use a minimum LWC threshold for cloud penetrations of  $0.25 \text{ g m}^{-3}$ , as measured by the CDP. This is the criterion used in two studies of cloud microphysics from the RICO campaign (Colón-Robles et al., 2006; Hudson and Mishra, 2007). These studies also required that updraft velocity be greater than 0.5 m/s, but we do not use that criterion because doing so would affect the updraft velocity distributions being used to run the model.

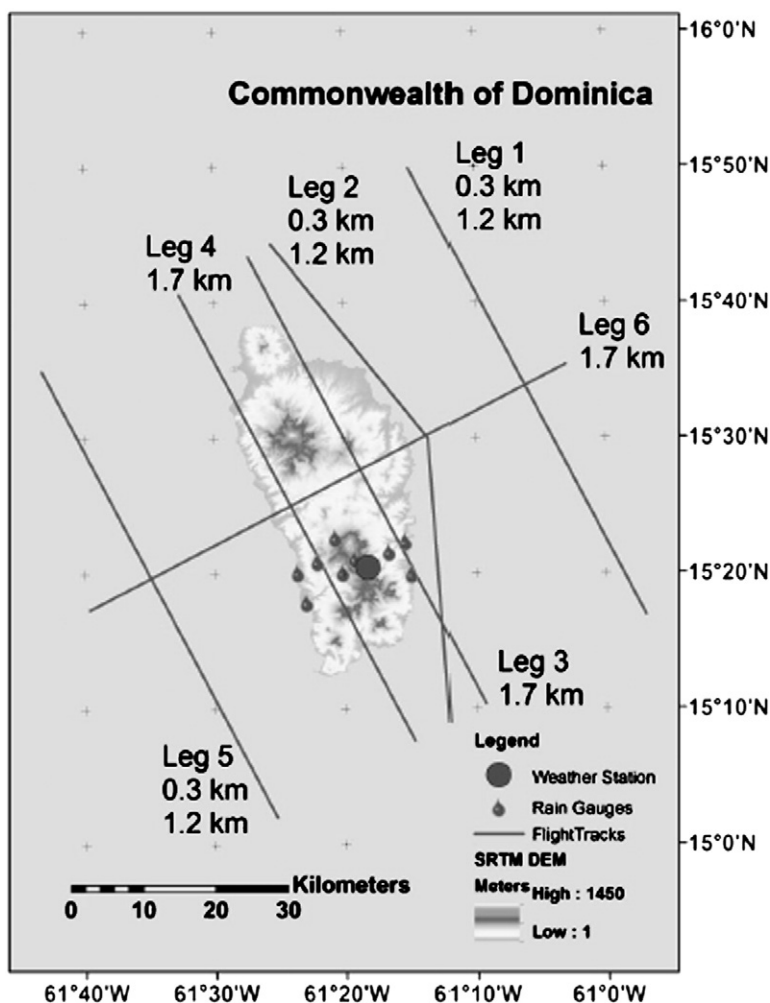


Fig. 1. Locations and altitudes of DOMEX flight legs, and terrain of Dominica. From (Smith et al., 2012).

### 3. Methods: defining simulation inputs

The version of the ARG model we use is the multiple aerosol types version, described in Abdul-Razzak and Ghan

(2000), which accepts as input several lognormal modes for the aerosol distribution. For each mode, the aerosol size distribution is defined through the median diameter, geometric standard deviation, and number concentration. Each

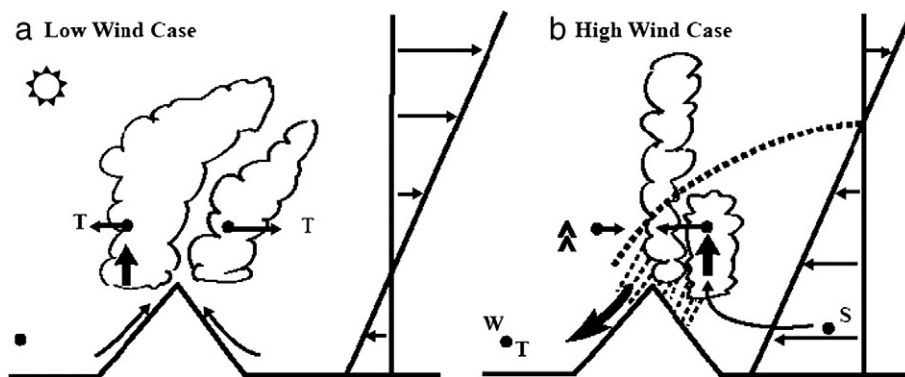


Fig. 2. Schematic of low wind (a) and high wind (b) convection regimes over Dominica. Trade wind profiles are shown to the right of the island. Thin curved arrows show cloud source air. Dots indicate flight legs. Convection is strongest near Leg 3 for the high wind case, and Leg 4 for the low wind case. From (Smith et al., 2012).

mode can contain one or multiple aerosol types, internally mixed; the fraction of each aerosol type within each mode, and the density and hygroscopicity of each aerosol type, must also be specified. The parameterization also requires a spectrum of cloud base updraft velocities, as well as other variables like temperature and pressure at the cloud base.

### 3.1. Aerosol size distribution

The CN and PCASP data provide information about the aerosol size distributions that can be used to construct lognormal modes in order to run the model. We use a uniform method across all flights for fitting the lognormal distributions to the observations for each flight. That method is described here.

The PCASP size distribution extends from 95 nm to 2.991  $\mu\text{m}$  in diameter, while the CN counter counts particles as small as 10 nm but does not record size distributions. By subtracting the total PCASP particle concentration from the CN particle concentration, an additional bin representing particles from 10 to 95 nm in diameter can be created. Thus we create a combined observed particle size distribution from the data from the two instruments. Fig. 3 shows an example of one of these size distributions for DOMEX flight RF13, a high wind case. As there are four maxima in the aerosol size distribution, we fit four modes to the data. We refer to them, from smallest to largest, as the Aitken mode, the accumulation mode, the coarse mode, and the giant mode.

The CN counter does not provide any information about the size distribution of the Aitken mode, so we must make assumptions about the median diameter and geometric standard deviation from this mode. We have assumed a median diameter of 40 nm for this mode. Field campaigns have observed Aitken mode median diameters close to this over the tropical ocean, but there is much variation; for example, the ACE-1, ACE-2 and Aerosols99 campaigns found Aitken mode median diameters of 44, 42, and 35 nm, respectively, for the subtropical Northern Hemisphere maritime boundary layer (Bates et al., 2002). The sensitivity of the model

results to changes in this assumption is tested in Section 5. For the geometric standard deviation, we use a value of 1.590, which is used in the CAM-Oslo GCM (Seland et al., 2008). Once these assumptions are made, the total Aitken mode concentration can be set so that the mode's particle concentration between 10 and 95 nm matches the CN bin concentration. Fig. 3 shows the fitted lognormal distribution for the Aitken mode, and the other three modes, superimposed above the observed aerosol size distribution.

For the other three modes, the PCASP data provide enough information to determine unique median diameters and geometric standard deviations for each flight. For lognormal aerosol modes, the geometric mean is the median diameter, and 84.1% of the particles are smaller than the product of the median diameter and geometric standard deviation (Seinfeld and Pandis, 2006). Hence, we calculate the median diameter and geometric standard deviation, as well as the particle number concentration, for the accumulation, coarse and giant modes using the PCASP bins between 95 and 491 nm, 491 nm and 1.191  $\mu\text{m}$ , and 1.191 and 2.991  $\mu\text{m}$ , respectively (these boundaries are the same for all flights). Where there is significant overlap between the modes, i.e. between the Aitken and accumulation modes and between the coarse and giant modes, the concentrations of particles from the smaller mode are subtracted from the PCASP bins for the larger mode before the fit for the larger mode is calculated.

In addition to the four individual modes, Fig. 3 shows the sum of the modes' aerosol concentrations. Comparing this sum to the observed size distribution, the fit seems reasonable where there is enough observational information about the aerosol size distribution. Table 1 shows the median diameter, standard deviation and total number concentration of each mode for the flight plotted in Fig. 3.

### 3.2. Aerosol composition

In the ARG parameterization, aerosol composition is handled through specification of the density and hygroscopicity of each aerosol type. The hygroscopicity is represented by the hygroscopicity parameter,  $B$ , which, for  $J$  internally mixed aerosol types, is defined as

$$B = \frac{\sum_{j=1}^J B_j q_j / \rho_j}{\sum_{j=1}^J q_j / \rho_j} \quad (1)$$

where  $B_j$  is the hygroscopicity parameter for aerosol type  $j$  (Abdul-Razzak and Ghan, 2000).

**Table 1**  
Lognormal fit parameters for RF13, an example DOMEX high wind flight, based on CN and PCASP data from Legs 1L and 1H.

Mode	Number conc. ( $\text{cm}^{-3}$ )	Median diam. (nm)	Geom. st. dev.
Aitken	188.72	40	1.590
Accumulation	73.70	173	1.324
Coarse	2.03	690	1.347
Giant	0.13	1690	1.282

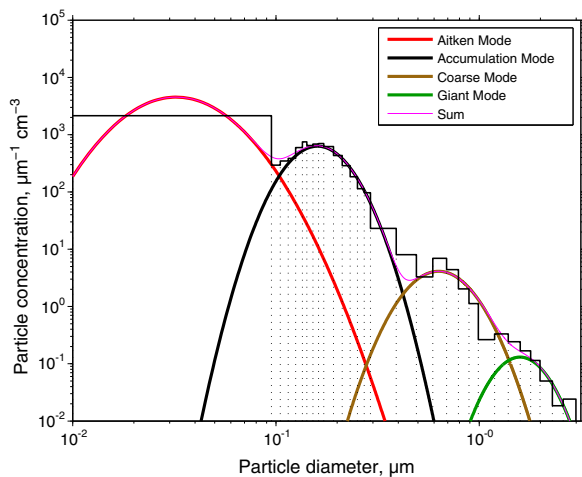


**Fig. 3.** Observed aerosol size distribution with fitted lognormal modes. X and Y axes on log scales. Observed distribution from CN and PCASP data from Leg 1 for RF13, an example DOMEX high wind case. Vertical lines show PCASP bin boundaries.

In this study, three aerosol types are used: sea salt (NaCl), ammonium sulfate, and organic carbon. The densities and hygroscopicity parameters used for each of these types are listed in Table 2. The values of  $B$  and  $\rho_a$  are based on those used in the MIRAGE model (Ghan et al., 2001).

### 3.3. Updraft velocities

The ARG parameterization considers variability in cloud base updraft velocity by integrating over a Gaussian probability density function (PDF) of updraft velocities. We have defined this spectrum using the mean and standard deviation of the observed in-cloud updraft velocities, including those data points from Leg 3 for the high wind flights, or Leg 4 for the low wind flights, with  $LWC > 0.25 \text{ g m}^{-3}$ .

One assumption implicit here is that the distribution of updraft velocities is actually Gaussian. Fig. 4 shows histograms of observed in-cloud updraft velocities for each flight. The histograms are normalized so that their area is 1. The Gaussian probability density functions with the means and standard deviations calculated from these data are superimposed over the histograms. The histogram is closest to a Gaussian distribution for RF08, which had the largest sample size: 338 data points (1 for each second with  $LWC > 0.25 \text{ g m}^{-3}$ ). Some of the other histograms appear slightly right-skewed, or bimodal, but overall the Gaussian spectrum appears to be a reasonable approximation of the updraft velocity distribution at flight level.

Another assumption is that the updraft velocity spectrum at flight level is representative of the spectrum at cloud base. This seems reasonable but there is no way to quantify the error in this assumption because we only have updraft velocity observations at one flight level. This issue presents a potential complication related to the negative updraft velocities included in the Gaussian distribution. When considering negative updraft velocities while integrating through the Gaussian PDF, the parameterization assumes that there are zero activated particles, because there would be negative vertical displacement and no adiabatic cooling. This limits the activation fraction predicted by our simulations to the fraction of positive updrafts in the spectrum. It could be argued that since all of the in-cloud air at flight level has been vertically displaced upward from the cloud base, it would not be valid to directly compare results from simulations assuming some negative updrafts to observations of cloud droplets taken in the clouds. However, entrainment of air into the clouds from the sides could mean that not all of the in-cloud air at flight level has been vertically displaced from cloud base. Still, to account for the possibility that all of the air in the clouds has actually been vertically displaced from the cloud base, we have run simulations with zero standard deviation in updraft velocity, and therefore no negative updrafts; see Section 6.1, a discussion on the role of the Aitken mode.

**Table 2**

Densities and hygroscopicities for aerosol types used in this study, based on values used in MIRAGE model (Ghan et al., 2001).

Component	$\rho_a \text{ (cm}^{-3}\text{)}$	$B$
Sea salt	2.17	1.146
Ammonium sulfate	1.769	0.507
Organic carbon	1.00	0.141

## 4. Control simulations

For the control simulations, for both the high wind and low wind cases, the aerosol size distributions for the four modes are fitted using the procedure described in Section 3.1. The Aitken and accumulation modes are assumed to consist entirely of ammonium sulfate, and the coarse and giant modes are assumed to consist entirely of sea salt. This is based on volatility measurements made during the RICO campaign, in a similar environment to the ocean near Dominica, which found that aerosols with diameters smaller than about  $0.4 \mu\text{m}$  were composed mainly of ammonium sulfate, while larger particles were composed mainly of sea salt (Peter et al., 2008; Hudson et al., 2011). The results of incorporating some organic carbon into the Aitken mode are discussed in Section 5.2.

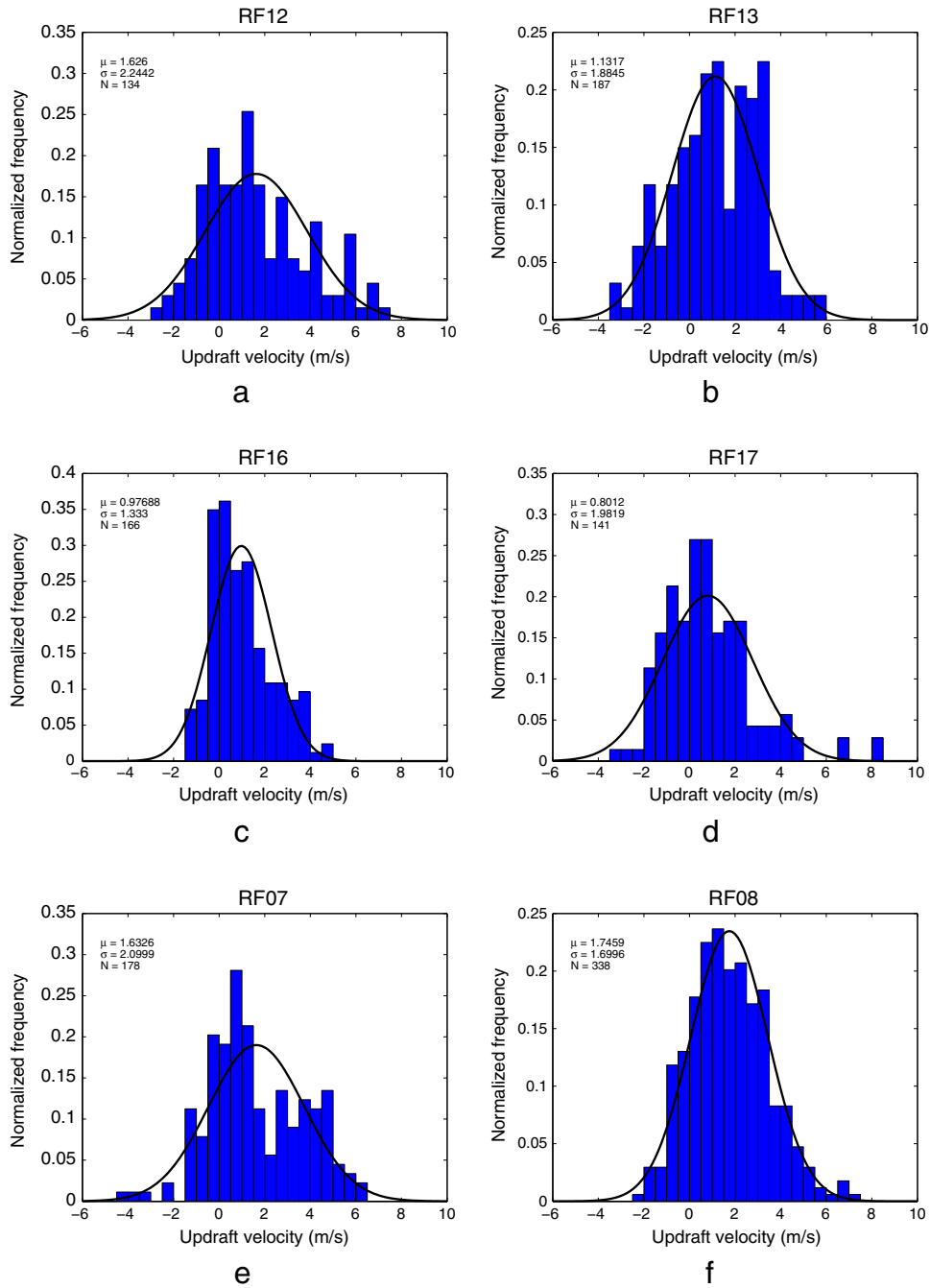
The cloud base temperature is assumed to be 293 K, since Leg 1L temperatures were typically about 297 or 298 K and the cloud base was typically about 400 to 500 m above Leg 1L's altitude. The cloud base temperature would need to be changed by on the order of 10 K, much greater than its uncertainty in DOMEEX, to produce changes comparable to those in the sensitivity tests described in Section 5.

Table 3 shows the results of the control simulations for each of the four DOMEEX high wind cases, RF12, RF13, RF16, and RF17, and the two low wind cases, RF07 and RF08. The results shown include the activation fraction and the cloud droplet number concentration (CDNC), broken down by aerosol mode. The observed droplet concentrations from CDP and FSSP, from Leg 3 for the high wind flights and Leg 4 for the low wind flights (see Section 2), are provided for comparison with the total simulated droplet concentration.

For the high wind cases, especially RF12, the simulation overestimates the observations by much more than the difference between the observed concentrations from the two instruments. Possible reasons for the discrepancy include the uncertainties explored in the sensitivity tests in Section 5, and the additional sources of error discussed in Section 6.2. The agreement is better for the low wind cases.

Table 3 also shows the mean and standard deviation of the Gaussian spectrum of updraft velocities fed to the parameterization; the ARG parameterization considers variability in updraft velocity by integrating over this spectrum. Since this sometimes results in negative vertical velocity, for which there can be no aerosol activation, the maximum possible activation fraction is the fraction of positive updraft velocities in the spectrum (see Section 3.3). Comparing the activation fractions for the individual modes to this theoretical maximum shows that effectively all of the particles for the giant and coarse modes, and almost all of the particles for the accumulation mode, are activated whenever there is an updraft. The Aitken mode, by contrast, has a much smaller activation fraction. However, since there are far more particles in the Aitken mode than in the other modes, the Aitken mode still accounts for a large fraction of the droplets, ranging from 42% to 45% for the low wind cases and 50% to 68% for the high wind cases. This would suggest that the Aitken mode is especially important in determining the droplet concentration in this setting. The coarse and giant modes, meanwhile, contribute no more than about 1% of the droplets. See Fig. 5 for pie charts showing the proportions





**Fig. 4.** Histograms and Gaussian PDFs for in-cloud updraft velocities for high-wind flights ((a) RF12, (b) RF13, (c) RF16, (d) RF17) and low-wind flights ((e) RF07, (f) RF08).

represented by each mode in the input aerosol particles, and the activated droplets.

### 5. Sensitivity tests

The sensitivity tests described here involve changing various assumptions or input parameters one at a time, and comparing the results to the control simulations. The cloud droplet concentrations resulting from all of these tests are

listed in Table 4, and selected results are shown in bar graphs in Fig. 6, for the high wind cases, and Fig. 7, for the low wind cases.

The observed droplet concentrations are included as well, but note that reconciling the model and observations is not a goal of these tests. Because the sensitivities represent unknown parameters, it would be impossible to tell whether the discrepancy was due to the modeling framework or the observations being wrong. In any case, the additional sources

**Table 3**

Updraft velocities, aerosol concentrations, activation fractions, and droplet concentrations from control simulations for DOMEX high and low wind cases, with observed droplet concentrations.

Flight	RF12	RF13	RF16	RF17	RF07	RF08
Mean in-cloud updraft velocity (m/s)	1.626	1.132	0.977	0.801	1.633	1.746
St. dev. in-cloud updraft velocity (m/s)	2.244	1.885	1.333	1.982	2.100	1.700
Aerosol conc.: Aitken mode ( $\text{cm}^{-3}$ )	309.17	188.72	194.21	242.13	734.32	977.22
Aerosol conc.: accumulation mode ( $\text{cm}^{-3}$ )	63.09	73.70	44.10	71.04	256.88	301.64
Aerosol conc.: coarse mode ( $\text{cm}^{-3}$ )	2.13	2.03	0.80	1.30	0.46	0.43
Aerosol conc.: giant mode ( $\text{cm}^{-3}$ )	0.13	0.13	0.06	0.10	0.002	0.02
Activation fraction: Aitken mode	0.3416	0.2896	0.3045	0.2541	0.2185	0.1866
Activation fraction: accumulation mode	0.7566	0.7162	0.7595	0.6480	0.7604	0.8324
Activation fraction: coarse mode	0.7647	0.7254	0.7674	0.6571	0.7803	0.8461
Activation fraction: giant mode	0.7648	0.7256	0.7674	0.6572	0.7807	0.8464
Fraction of positive updrafts	0.7656	0.7259	0.7682	0.6570	0.7816	0.8478
Droplet conc.: Aitken mode ( $\text{cm}^{-3}$ )	105.61	54.64	59.14	61.52	160.43	182.31
Droplet conc.: accumulation mode ( $\text{cm}^{-3}$ )	47.73	52.78	33.50	46.03	195.34	251.10
Droplet conc.: coarse mode ( $\text{cm}^{-3}$ )	1.63	1.47	0.62	0.86	0.36	0.37
Droplet conc.: giant mode ( $\text{cm}^{-3}$ )	0.10	0.10	0.05	0.07	0.001	0.02
Droplet conc.: total ( $\text{cm}^{-3}$ )	155.06	108.99	93.30	108.47	356.13	433.80
Observed droplet conc.: CDP ( $\text{cm}^{-3}$ )	88.13	90.68	64.68	75.00	313.34	393.27
Observed droplet conc.: FSSP ( $\text{cm}^{-3}$ )	90.34	95.02	71.97	82.43	331.05	406.00

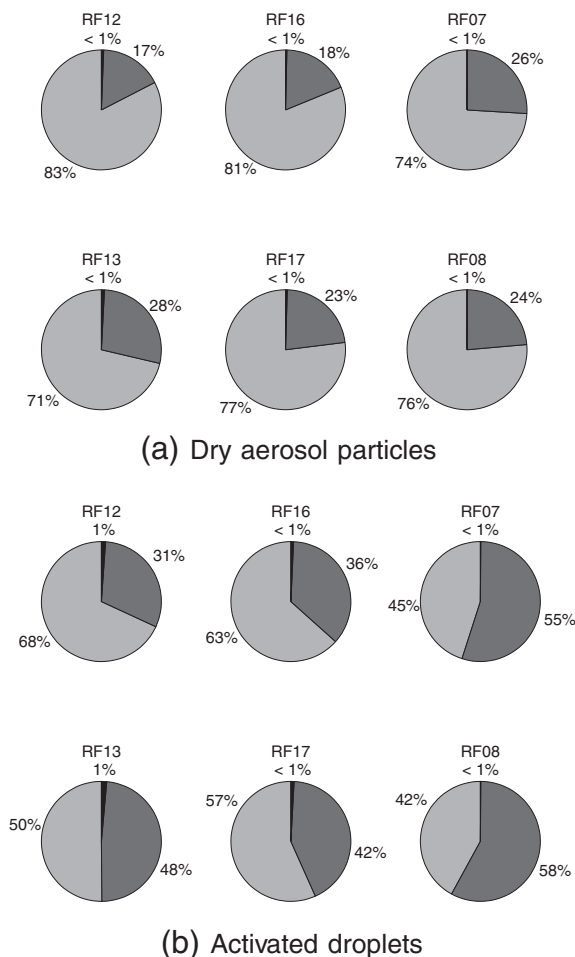


**Fig. 5.** Fractions of (a) aerosol particles and (b) activated droplets contributed by each mode, in control simulations of droplet activation for DOMEX high wind cases (RF12, RF13, RF16, and RF17) and low wind cases (RF07 and RF08). Light gray: Aitken mode; dark gray: accumulation mode; black: coarse and giant modes.

of error described in Section 6.2 make our setup unsuitable for evaluating the accuracy of the ARG parameterization, which is already well understood (Nenes and Seinfeld, 2003; Rissman et al., 2004; Ghan et al., 2011). The sensitivity tests are more useful for determining what factors are most important in determining the activation fraction over Dominica, and what types of observations are most important for predicting that fraction.

The observed values are, rather, provided to show whether the model is a reasonable framework for investigating these questions. For the low wind flights, the model agrees well with the observations in the control simulations, leading to a greater degree of confidence regarding conclusions about the sensitivities. For the high wind flights, especially RF12 and RF16, the model more substantially overpredicts the observed droplet concentrations; for RF12, the discrepancy is too large to be accounted for by any of the sensitivity tests in this section. The sources of error discussed in Section 6.2 may account for the remaining discrepancy for RF12 and for the consistent overestimation for the high wind flights, but since these sources of error reflect physical processes not considered by the model, we must be more careful when drawing conclusions about the real-world sensitivities for the high wind regime.

### 5.1. Aitken mode median diameter

Since the Aitken mode's median diameter cannot be determined based on DOMEX observations and must be assumed, it is important to test sensitivity of the model results to changes in this parameter. We have run simulations with the Aitken mode median diameter changed from 40 nm to 44 nm and 36 nm. The lognormal fits for the other modes are recalculated based on this changed assumption. The results of this test are summarized in Table 4 and also appear in Figs. 6 and 7.

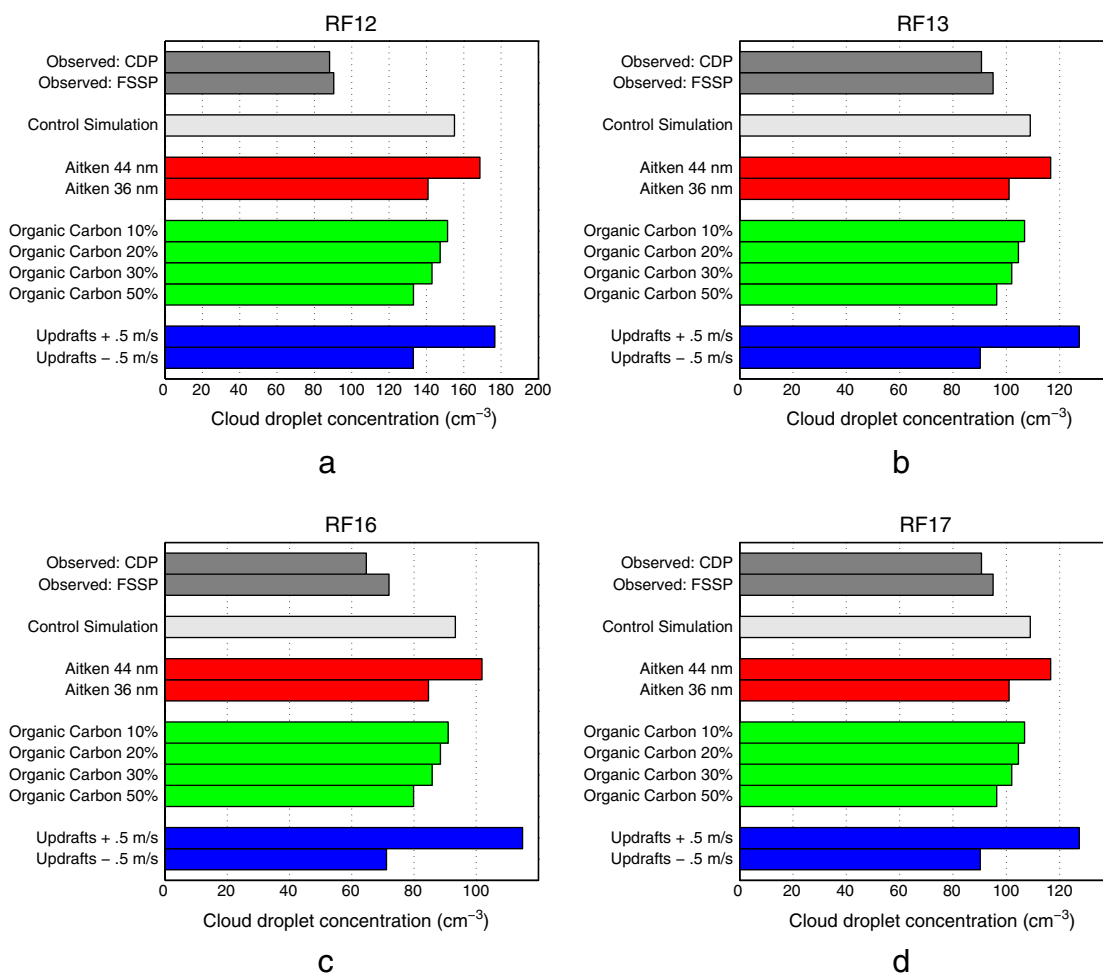
The change in the simulated droplet concentration from this test is significant: between about 8 and 13  $\text{cm}^{-3}$  for the

**Table 4**Total droplet concentrations, in  $\text{cm}^{-3}$ , from all sensitivity tests for high and low wind cases, with control simulations and observations.

Flight		RF12	RF13	RF16	RF17	RF07	RF08
Observed	CDP	88.13	90.68	64.68	75.00	313.34	393.27
	FSSP	90.34	95.02	71.97	82.43	331.05	406.00
Control simulation		155.06	108.99	93.30	108.47	356.13	433.80
Aitken mode median diameter	44 nm	168.66	116.61	101.87	117.24	383.08	472.08
	36 nm	140.86	101.03	84.68	99.52	328.32	397.50
Organic carbon internally mixed	5%	153.23	107.93	92.16	107.28	352.19	428.67
	10%	151.34	106.83	90.99	106.05	348.15	423.43
	15%	149.37	105.70	89.77	104.77	344.00	418.06
	20%	147.32	104.52	88.52	103.45	339.73	412.58
	25%	145.19	103.29	87.21	102.07	335.34	406.96
	30%	142.97	102.02	85.85	100.65	330.82	401.22
Mean updraft velocity	50%	133.07	96.41	79.86	94.36	311.33	376.80
	+ 0.5 m/s	176.66	127.35	114.89	129.52	405.00	494.47
	− 0.5 m/s	133.03	90.23	71.17	87.89	305.78	369.38

high wind flights, and between about 27 and 39  $\text{cm}^{-3}$  for the low wind flights, from a change of 4 nm in the Aitken mode median diameter. Aitken mode median diameters of 44 or 36 nm are also plausible values for the Aitken mode median

diameter. This suggests that the size distribution of particles in the Aitken mode is very important in determining the overall aerosol activation fraction in this setting, and shows that the lack of observations of the size distribution

**Fig. 6.** Results of sensitivity tests for high wind cases: (a) RF12, (b) RF13, (c) RF16, and (d) RF17. See also Table 4.



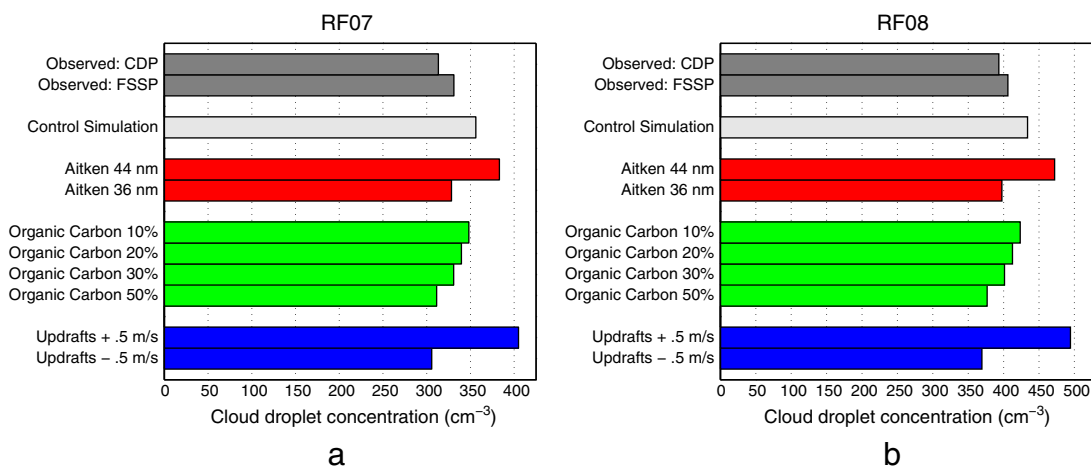


Fig. 7. Results of sensitivity tests for low wind cases: (a) RF07, and (b) RF08. See also Table 4.

of particles smaller than 95 nm presents a limitation on our ability to accurately predict the observed droplet concentration.

### 5.2. Aitken mode composition

Since the Aitken mode composition is unknown, we have tried incorporating various amounts of organic carbon into the mode. Table 4 shows the results from incorporating 5%, 10%, 15%, 20%, 25%, 30%, and 50% by volume organic carbon, internally mixed, in the Aitken mode for the six DOMEX example flights. The 10%, 20%, 30%, and 50% cases are shown in the bar graphs in Figs. 6 and 7. Fuentes et al. (2011) found organic mass fractions on the order of 8% to 37% in submicron aerosols from seawater proxies enriched in organic material from phytoplankton cultures, and Dowd et al. (2004) found that submicron aerosol over the North Atlantic may be as high as 63% organic by mass in times of high biological activity, so the organic fractions tested here are plausible, although 50% may be near the upper extreme. The effects of these changes on the droplet concentration are of similar magnitude to those from the Aitken mode median diameter test, suggesting that the composition of small particles, as well as their size distribution, is important for the overall aerosol activation fraction in this setting.

### 5.3. Mean updraft velocity

Uncertainty in the updraft velocity observations comes partly from changes in the amount of fuel remaining in the aircraft during flight, which affected the aircraft's weight and hence the flow patterns around the aircraft, creating a time-varying bias in the  $w$  observations. By comparing the raw values of  $w$  with a high-pass filtered version, the instantaneous uncertainty in the measurements could be estimated to be about  $\pm 0.25$  m/s. The in-cloud leg average carries some additional uncertainty associated with the choice of the criterion for cloud penetrations, so we estimate the error in the mean in-cloud updraft velocities used in the simulations to be on the order of  $\pm 0.5$  m/s. We have tested the sensitivity of the simulated droplet concentration to adding or subtracting 0.5 m/s to the

mean updraft velocity for each flight. The results from this test are summarized in Table 4 and also appear in Figs. 6 and 7.

Higher updraft velocities lead to more particles activated. This result is expected from theory: stronger updrafts lead to faster adiabatic cooling, limiting the amount of water vapor that can diffuse to larger particles and leading to higher supersaturations, activating smaller particles. The effect of this change in updraft velocity on the model results is relatively large, causing a difference of about 18 to 22 droplets per cubic centimeter.

## 6. Discussion

### 6.1. Role of Aitken mode

While in many situations the accumulation mode is most important in determining the cloud droplet concentration, our simulations suggest that over Dominica, for both the low and high wind cases, the Aitken mode is also very important, and in some respects is more important than the accumulation mode.

There are several possible meanings of the relative importance of different modes. One is concerned with which mode is most responsible for the shifts in activated droplet concentration in the sensitivity tests. By this measure the Aitken mode is especially important. Fig. 8 shows the concentration of activated droplets from the Aitken and accumulation modes in RF13, in simulations with updraft velocities from 0.0 to 2.0 m/s, with zero standard deviation of updraft velocity, and otherwise identical to the control case. As the updraft velocity is ramped up from 0 to 0.1 m/s, almost no Aitken mode particles are activated, and the number of activated droplets in the accumulation mode rises sharply. However, with further increases in updraft velocity, the rate of increase of activated droplets in the accumulation mode slows down as the mode nears saturation (when all of the particles are activated), and the Aitken mode starts to contribute more significantly to the activated droplets. For updraft velocities larger than about 0.3 m/s, effectively all of the particles in the accumulation mode are activated ( $73.70 \text{ cm}^{-3}$ ), and the response of the total droplet concentration to changes in the updraft velocity is entirely due to

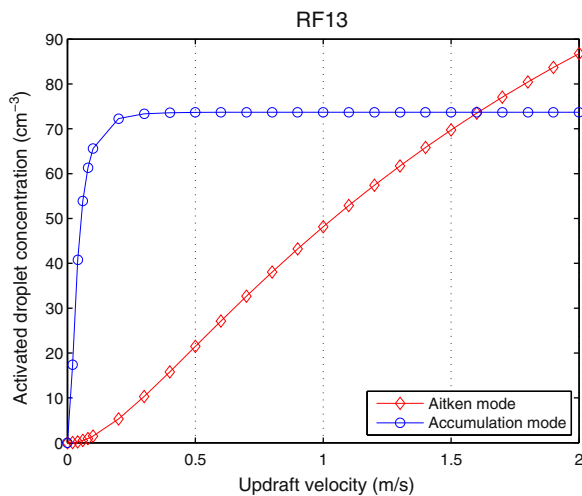


**Fig. 8.** Activated droplets from the Aitken and accumulation modes for RF13, with single updraft velocities from 0 to 0.1 m/s in increments of 0.02, and from 0.1 to 2.0 m/s in increments of 0.1. The coarse and giant modes are not plotted because their number concentrations are very small.

changes in the number of Aitken mode particles activated. The mean in-cloud updraft velocities observed during DOMEX are on the order of 1 m/s, well within the region where the Aitken mode is responsible for changes in the simulated droplet concentration due to small changes in updraft velocity, or to the other types of perturbations involved in the sensitivity tests in Section 5.

Another measure of the importance of the modes is simply the fraction of activated droplets contributed by each mode. The pie charts in Fig. 5 show that, in our control simulations, the Aitken mode accounts for half to two thirds of the activated droplets in the high wind regime and almost half in the low wind regime, indicating that in some circumstances the Aitken mode is “most important” even by this measure.

If the limitation on the activation fraction imposed by negative updrafts (see Section 3.3 and Table 3) was removed, the accumulation mode could account for more of the activated droplets. To investigate this possibility, we have run simulations identical to the control simulations but with half of the observed standard deviation of updraft velocity, and therefore fewer negative updrafts, and with zero standard deviation, and therefore no negative updrafts. These simulations were run twice, once with the Aitken mode still included in the simulations, and once with the Aitken mode removed completely, to impose the constraint that none of the Aitken mode particles are activated. Table 5 shows the results of these simulations, which address the question of whether the inclusion of the Aitken mode is necessary to explain the observed droplet concentrations, and help to illustrate the effects of competition for water vapor between the different modes.

For the simulations with the Aitken mode included, Table 5 shows, in addition to the total predicted droplet concentrations, the concentrations from only the accumulation and larger modes. Comparison of these results with those of the simulations from which the Aitken mode was left out

entirely illustrates several secondary effects of the removal of the Aitken mode. In the control case, the numerous Aitken mode particles that do not become activated still compete for water vapor, so removing these particles results in artificially high supersaturations and higher activation fractions in the accumulation mode. Also, for the simulations without the Aitken mode, the fits for the other three modes were recalculated based only on the PCASP data; this resulted in more particles in the accumulation mode, because there was no subtraction from the PCASP bins due to the overlapping Aitken mode.

Reducing the standard deviation of  $w$  reduces the frequency of small and negative updrafts but also of strong updrafts, so it could result in higher or lower droplet concentrations, but Table 5 shows an increase in the predicted droplet concentration in every case but one. The exception is for RF17 with the Aitken mode included, where the droplet concentration decreases slightly when the standard deviation of  $w$  is halved. Despite this, the droplet concentration from the accumulation and larger modes increases in this case. This is an interesting example of competition between the different modes: while more of the larger particles are activated, the Aitken mode's activation fraction goes down by just more than enough to compensate.

The fact that the simulations without the Aitken mode underestimate the observed droplet concentrations in almost all cases suggests that Aitken mode particles were likely activated during DOMEX. This argument can also be made from the aerosol observations themselves. For the “Zero  $w$  SD” case with the Aitken mode excluded (see last row of Table 5), the activation fraction is nearly 100%, and the concentrations of activated droplets from these simulations match the total particle concentrations from PCASP used to define the lognormal modes to within 0.2%. If the observations had zero uncertainty, this would mean that for all the flights except RF17, it would be impossible to account for the observed droplet concentrations without activating particles smaller than  $0.095 \mu\text{m}$ , the lower detection limit for PCASP. In reality, the observations do have some uncertainty on the order of these underestimations, so the possibility that none of these small particles were activated on any of the flight days cannot be definitively ruled out. However, this would require several contingencies which seem unlikely: that all of the particles in the larger modes were activated, despite entrainment of dry air and competition from the Aitken mode, and that the measurements consistently underestimated the concentrations of larger particles, or overestimated the cloud droplet concentrations, by enough to close the remaining gap.

It is worth noting that for all of the simulations in Table 5, even the control simulation (the “Full obs.  $w$  SD” case with the Aitken mode included), the droplets activated from the accumulation and larger modes account for more than half of the *observed* droplet concentration, even if the Aitken mode accounts for a majority of the *simulated* droplet concentration (see Fig. 5). If the model's overestimation of the observed droplet concentration is due to too many Aitken mode particles being activated, i.e. if these particles were actually smaller or less hygroscopic than they were assumed to be, then the Aitken mode would be less important in terms of the contribution to the total droplet concentration than Fig. 5 would suggest.

The importance of small particles may be due to the high updraft velocities, relative to oceanic cumulus, caused by

**Table 5**

Concentrations of activated droplets, in  $\text{cm}^{-3}$ , for simulations in which the standard deviation  $w$  was reduced to half of the observed value ("Half obs. w SD"), or to 0 ("Zero w SD"). These were run twice, once with the Aitken mode included in the simulation, as in the control case, and once with the Aitken mode excluded from the simulation. For the runs with the Aitken mode included, two droplet concentrations are given: the total activated droplet concentration and the concentration of activated droplets from the accumulation, coarse and giant modes only. Observed droplet concentrations are included for comparison. The "Full obs. w SD" case with the Aitken mode included is identical to the control case (compare third row of this table with third-to-last row of Table 3). The droplet concentrations in the "Zero w SD" case with the Aitken mode excluded (last row) match the PCASP aerosol observations used to define the lognormal modes to within 0.2%.

Flight		RF12	RF13	RF16	RF17	RF07	RF08
Observed droplet conc.	CDP	88.13	90.68	64.68	75.00	313.34	393.27
	FSSP	90.34	95.02	71.97	82.43	331.05	406.00
Aitken mode in simulation,	Full obs. w SD	155.06	108.99	93.30	108.47	356.13	433.80
full activated droplet conc.	Half obs. w SD	166.32	117.54	99.60	108.38	386.28	468.13
	Zero w SD	181.38	130.21	107.42	122.53	410.81	479.69
Aitken mode in simulation,	Full obs. w SD	49.45	54.35	34.16	46.95	195.70	251.49
droplet conc. excluding	Half obs. w SD	59.90	66.18	41.35	56.15	236.29	293.59
Aitken mode	Zero w SD	65.34	75.86	44.97	72.44	256.94	302.10
Aitken mode excluded	Full obs. w SD	56.42	58.49	38.65	51.77	213.41	273.50
from simulation	Half obs. w SD	68.41	71.33	46.82	62.05	257.91	319.03
	Zero w SD	74.95	81.72	51.00	79.96	279.94	329.44

Dominica's orographic setting, which allows for higher supersaturations, activating smaller particles. While the work of Reutter et al. (2009) suggested that particle composition is important in determining droplet concentration only for very low supersaturations, Ward et al. (2010) found that composition may also be important at high supersaturations in situations where the median aerosol diameter is small. The sensitivity to different fractions of organic carbon in our simulations suggests that orographic precipitation over Dominica is one setting where that conclusion applies.

### 6.2. Additional sources of error for high wind cases

Apart from the independent variables for the sensitivity tests in this study, one possible reason for the model's overestimation of the observed droplet concentration, for the high wind case, is pre-existing clouds upwind of Dominica. Upwind clouds were found in the DOMEX high wind flights (Smith et al., 2012), but the ARG model assumes that the initial air parcel is cloud-free. If air from pre-existing clouds became mixed into the cloud-free air used to define the aerosol size distribution, the pre-existing droplets would grow quickly once lifted, leading to lower supersaturations and droplet concentrations lower than the model predictions.

Another possible explanation for this overestimation is removal of water droplets through precipitation, which would lower the observed droplet concentration. There was almost no precipitation on the low wind days (and, in fact, almost no climatological diurnal cycle in precipitation over Dominica) (Smith et al., 2012), so this would only be an issue for the high wind cases.

A third source of error is entrainment of subsaturated air into the clouds, which is not considered by the model. We have tried raising the LWC criterion for defining clouds in order to sample away from cloud edges, but while this reduced the observed droplet concentration, the simulated concentration increased by more than enough to compensate due to higher updraft velocities in the cloud cores.

Among the high wind flights, RF12 in particular stands out in the amount by which the simulation overestimates the observed droplet concentration, and in the number of particles

in the Aitken mode; we suspect that these are connected. One possible explanation for the large number of small particles for this flight is the emission of small black carbon particles, possibly by passing ships. Another possibility is a recent particle formation event, involving sulfuric acid nucleating from the gas phase, which could have occurred just before the flight: this could account for many particles which would be too small to contribute significantly to droplet activation.

With the exception of entrainment, these issues do not apply to the low wind cases. Our results for the low wind cases suggest that using ammonium sulfate for the Aitken and accumulation modes, with a small amount of organic carbon in the Aitken mode, would work well for modeling droplet activation in a tropical, island, orographic, thermally-driven setting.

### 6.3. Suggestions for future measurements

The results of the sensitivity tests provide insights into what observational information is most relevant for modeling studies of aerosol activation in a tropical, orographic setting. In particular, they suggest that aerosol composition and size distribution at small particle sizes (less than 100 nm in diameter) are important in this setting. Future observational campaigns in regimes with strong updrafts may benefit from the inclusion of instruments to measure the size distribution of small particles and to determine their composition.

One example of a similar study involving such measurements is the aerosol-CDNC closure study by Conant et al. (2004), which used aerosol, updraft and thermodynamic observations from the CRYSTAL-FACE campaign over Florida to predict cloud droplet number concentration in cumulus clouds using the parcel model described in Nenes et al. (2002). Their predicted droplet concentrations matched the observations to within 15% on average, using assumptions for aerosol composition similar to ours (ammonium bisulfate for submicron modes and NaCl for supermicron modes). The CRYSTAL-FACE campaign used a Dual Automatic Classifier Detector System (DACADS) instrument, in addition to the PCASP, to measure the size distribution of aerosols down to diameters of 15 nm, eliminating the need for sensitivity tests to the sizes of small particles. Also on board was a mass

spectrometer which identified organic carbon and sulfate ions, helping to identify the composition of the aerosols, although some sensitivity tests for composition were still necessary due to remaining uncertainty.

## 7. Conclusions

We have used data for aerosol size distributions and updraft velocities from the DOMEX campaign to simulate the process of aerosol activation in orographic clouds over the island of Dominica. We used a parcel model incorporating the Abdul-Razzak and Ghan (2000) parameterization of aerosol activation and assumed that small particles were composed of ammonium sulfate and large particles of sea salt. These simulations tended to overestimate the observed cloud droplet number concentrations, especially for days with strong trade winds, but in most cases the discrepancies were smaller than the sensitivity of our simulated droplet concentrations to changes in our inputs on the order of their uncertainty. Possible sources of error not addressed by our sensitivity tests include entrainment, precipitation, and pre-existing clouds upwind of Dominica.

Our sensitivity tests have shown that the mean updraft velocity is a major controlling factor of the droplet concentration, with stronger updrafts leading to higher maximum supersaturations and more activated droplets, as expected from theory. More interestingly, the Aitken mode appears to play an important role in determining the activation fraction and droplet concentration in this setting. Activated droplets from these particles accounted for 42% to 68% of the total droplet concentration in our control simulations. While the overestimation of the observed droplet concentration suggests that our simulations may have activated too many particles from the Aitken mode, simulations entirely excluding the Aitken mode consistently underestimated the observed droplet concentration, except for flight RF17 in the extreme case of no w variance. The Aitken mode is especially important in the sense that changes in the total CDNC in our sensitivity tests are dominated by changes in the number of droplets activated from the Aitken mode.

Our lack of observations of the sizes and compositions of particles smaller than 100 nm prevented us from further constraining the role of the Aitken mode or predicting the observed droplet concentration with more precision. Future field campaigns in areas where the Aitken mode might be important for cloud droplet activation, such as regimes with strong updrafts and a relative abundance of small particles, should benefit from the inclusion of instruments to better characterize these particles' size distribution and chemical composition.

## Acknowledgments

Two anonymous reviewers provided constructive comments which helped to improve the paper. Jeffrey French of the University of Wyoming provided useful guidance regarding the uncertainty in the DOMEX measurements.

## References

Abdul-Razzak, H., Ghan, S.J., 2000. A parameterization of aerosol activation 2. Multiple aerosol types. *J. Geophys. Res.* 105, 6837–6844.

- Abdul-Razzak, H., Ghan, S.J., Rivera-Carpio, C., 1998. A parameterization of aerosol activation 1. Single aerosol type. *J. Geophys. Res.* 103, 6123–6131.
- Albrecht, B.A., 1989. Aerosols, cloud microphysics, and fractional cloudiness. *Science* 245, 1227–1230.
- Bates, T.S., Coffman, D.J., Covert, D.S., Quinn, P.K., 2002. Regional maritime boundary layer aerosol size distributions in the Indian, Atlantic and Pacific Oceans: a comparison of INDOEX measurements with ACE-1, ACE-2, and Aerosols99. *J. Geophys. Res.* 107, 8026.
- Colón-Robles, M., Rauber, R.M., Jensen, J.B., 2006. Influence of low-level wind speed on droplet spectra near cloud base in trade wind cumulus. *Geophys. Res. Lett.* 33, L20814.
- Conant, W.C., VanReken, T.M., Rissman, T.A., Varutbangkul, V., Jonsson, H.H., Nenes, A., Jimenez, J.L., Delia, A.E., Bahreini, R., Roberts, G.C., Flagan, R.C., Seinfeld, J.H., 2004. Aerosol-cloud drop concentration closure in warm cumulus. *J. Geophys. Res.* 109, D13204.
- Forster, P., Ramaswamy, V., Artaxo, P., Bernsten, T., Betts, R., Fahey, D., Haywood, J., Lean, J., Lowe, D.C., Myhre, G., Nganga, J., Prinn, R., Raga, G., Schulz, M., Van Dorland, R., 2007. Changes in atmospheric constituents and in radiative forcing. *Climate Change 2007: The Physical Science Basis*. Cambridge University Press, pp. 129–234.
- Fuentes, E., Coe, H., Green, D., McFiggans, G., 2011. On the impacts of phytoplankton-derived organic matter on the properties of the primary marine aerosol—Part 2: Composition, hygroscopicity and cloud condensation activity. *Atmos. Chem. Phys.* 11, 2585–2602.
- Ghan, S.J., Abdul-Razzak, H., Nenes, A., Ming, Y., Liu, X., Ovchinnikov, M., Shipway, B., Meskhidze, N., Xu, J., Shi, X., 2011. Droplet nucleation: Physically-based parameterizations and comparative evaluation. *J. Adv. Model. Earth Syst.* 3, M10001.
- Ghan, S.J., Laulainen, N., Easter, R., Wagoner, R., Nemesure, S., Chapman, E., Zhang, Y., Leung, R., 2001. Evaluation of aerosol direct radiative forcing in MIRAGE. *J. Geophys. Res.* 106, 5295–5316.
- Hudson, J.G., Mishra, S., 2007. Relationships between CCN and cloud microphysics variations in clean maritime air. *Geophys. Res. Lett.* 34, L16804.
- Hudson, J.G., Noble, S., Jha, V., 2011. On the relative role of sea salt cloud condensation nuclei (CCN). *J. Atmos. Chem.* 68, 71–88.
- Köhler, H., 1921. Zur kondensation des wassers in der atmosphäre. *Meteorologische Zeitschrift* 38, 168–171.
- Lohmann, U., Feichter, J., 2005. Global indirect aerosol effects: a review. *Atmos. Chem. Phys.* 5, 715–737.
- Nenes, A., Charlson, R.J., Facchini, M.C., Kulmala, M., Laaksonen, A., Seinfeld, J.H., 2002. Can chemical effects on cloud droplet number rival the first indirect effect? *Geophys. Res. Lett.* 29, 1848.
- Nenes, A., Seinfeld, J.H., 2003. Parameterization of cloud droplet formation in global climate models. *J. Geophys. Res.* 108, 4415.
- O'Dowd, C.D., Facchini, M.C., Cavalli, F., Ceburnis, D., Mircea, M., Decesari, S., Fuzzi, S., Yoon, Y.J., Putaud, J.P., 2004. Biogenically driven organic contribution to marine aerosol. *Nature* 431, 676–680.
- Peter, J.R., Blyth, A.M., Brooks, B., McQuaid, J.B., Lingard, J.J.N., Smith, M.H., 2008. On the composition of caribbean maritime aerosol particles measured during RICO. *Q. J. R. Meteorol. Soc.* 134, 1059–1063.
- Ramaswamy, V., Boucher, O., Haigh, J., Hauglustaine, D., Haywood, J., Myhre, G., Nakajima, T., Shi, G., Solomon, S., 2001. Radiative forcing of climate change. *Climate Change 2001: The Scientific Basis*. Cambridge University Press, pp. 349–416.
- Reutter, P., Su, H., Trentmann, J., Simmel, M., Rose, D., Gunthe, S.S., Wernli, H., Andreae, M.O., Pöschl, U., 2009. Aerosol- and updraft-limited regimes of cloud droplet formation: influence of particle number, size and hygroscopicity on the activation of cloud condensation nuclei (CCN). *Atmos. Chem. Phys.* 9, 7067–7080.
- Rissman, T.A., Nenes, A., Seinfeld, J.H., 2004. Chemical amplification (or dampening) of the Twomey effect: conditions derived from droplet activation theory. *J. Atmos. Sci.* 61, 919–930.
- Seinfeld, J.H., Pandis, S.N., 2006. *Atmospheric Chemistry and Physics: From Air Pollution to Climate Change*, Second edition. John Wiley and Sons, New York.
- Seland, Ø., Iversen, T., Kirkevåg, A., Storelvmo, T., 2008. Aerosol-climate interactions in the CAM-Oslo atmospheric GCM and investigation of associated basic shortcomings. *Tellus* 60A, 459–491.
- Smith, R.B., Minder, J.R., Nugent, A.D., Storelvmo, T., Kirshbaum, D.J., Warren, R., Lareau, N., Palany, P., James, A., French, J., 2012. Orographic precipitation in the tropics: the Dominica Experiment. *Bull. Am. Meteorol. Soc.* 93, 1567–1579.
- Strapp, J.W., Leaith, W.R., Liu, P.S.K., 1992. Hydrated and dried aerosol-size-distribution measurements from the Particle Measuring Systems FSSP-300 probe and the deiced PCASP-100X probe. *J. Atmos. Ocean. Technol.* 9, 548–555.
- Twomey, S., 1974. Pollution and the planetary albedo. *Atmos. Environ.* 8, 1251–1256.
- Ward, D.S., Eidhammer, T., Cotton, W.R., Kreidenweis, S.M., 2010. The role of the particle size distribution in assessing aerosol composition effects on simulated droplet activation. *Atmos. Chem. Phys.* 10, 5435–5447.